Radiation Protection and Occupational Exposure on ^{68}Ga-PSMA-11–Based Cerenkov Luminescence Imaging Procedures in Robot-Assisted Prostatectomy

Pedro Fragoso Costa[1,2], Wolfgang P. Fendler[1,2], Ken Herrmann[1,2], Patrick Sandach[1,2], Hong Grafe[1,2], Maarten R. Grootendorst[3], Lukas Püllen[2,4], Claudia Kesch[2,4], Ulrich Krafft[2,4], Jan P. Radtke[2,4], Stephan Tschirdewahn[2,4], Boris A. Hadaschik[2,4], and Christopher Darr[2,4]

[1]Department of Nuclear Medicine, University Hospital Essen, Essen, Germany; [2]German Cancer Consortium (DKTK)-University Hospital Essen, Essen, Germany; [3]Clinical Department, Lightpoint Medical Ltd., Chesham, United Kingdom; and [4]Department of Urology and Urological Oncology, University Hospital Essen, Essen, Germany

Cerenkov luminescence imaging (CLI) was successfully implemented in the intraoperative context as a form of radioguided cancer surgery, showing promise in the detection of surgical margins during robot-assisted radical prostatectomy. The present study was designed to provide a quantitative description of the occupational radiation exposure of surgery and histopathology personnel from CLI-guided robot-assisted radical prostatectomy after the injection of ^{68}Ga-PSMA-11 in a single-injection PET/CT CLI protocol. **Methods:** Ten patients with preoperative ^{68}Ga-PSMA-11 administration and intraoperative CLI were included. Patient dose rate was measured before PET/CT ($n = 10$) and after PET/CT ($n = 5$) at a 1-m distance for 4 patient regions (head [A], right side [B], left side [C], and feet [D]). Electronic personal dosimetry (EPD) was used for intraoperative occupational exposure ($n = 10$). Measurements included the first surgical assistant and scrub nurse at the operating table and the CLI imager/surgeon at the robotic console and encompassed the whole duration of surgery and CLI image acquisition. An estimation of the exposure of histopathology personnel was performed by measuring prostate specimens ($n = 8$) with a germanium detector. **Results:** The measured dose rate value before PET/CT was 5.3 ± 0.9 (average $\pm$ SD) μSv/h. This value corresponds to a patient-specific dose rate constant for positions B and C of 0.047 μSv/h·MBq. The average dose rate value after PET/CT was 1.04 ± 1.00 μSv/h. The patient-specific dose rate constant values corresponding to regions A to D were 0.011, 0.026, 0.024, and 0.003 μSv/h·MBq, respectively. EPD readings revealed average personal equivalent doses of 9.0 ± 7.1, 3.3 ± 3.9, and 0.7 ± 0.7 μSv for the first surgical assistant, scrub nurse, and CLI imager/surgeon, respectively. The median germanium detector–measured activity of the prostate specimen was 2.96 kBq (interquartile range, 2.23–7.65 kBq). **Conclusion:** Single-injection ^{68}Ga-PSMA-11 PET/CT CLI procedures are associated with a reasonable occupational exposure level, if kept under 110 procedures per year. Excised prostate specimen radionuclide content was below the exemption level for ^{68}Ga. Dose rate–based calculations provide a robust estimation for EPD measurements.

Key Words: Cerenkov luminescence imaging; radioguided surgery; prostate cancer; margin assessment; radical prostatectomy

J Nucl Med 2022; 63:1349–1356
DOI: 10.2967/jnumed.121.263175

In men with local prostate cancer (PC), surgery or radiotherapy is the treatment modality of choice. Radical prostatectomy (RP) with complete removal of the prostate and the PC aims to cure the patient; however, collateral damage, such as impotence and incontinence, may occur. These problems greatly impair the quality of life, so that in the context of RP, the anatomic structures for continence and potency should be spared as much as possible (*1*). In this regard, positive resection margins (PSM) may occur in nerve-sparing RP or in locally advanced PC. The presence of PSM is associated with an increased risk of biochemical recurrence (*2*). In addition, the risk of metastasis is increased with PSM of greater than 2 mm or multiple PSM. Preoperative MRI and prostate sampling with systematic and fusion-guided biopsy cores help to guide neurovascular bundle preservation planning without increasing the risk and number of PSM (*3–5*). Intraoperative frozen-section analysis can help the surgeon to preserve these structures (*1,6*). However, besides resource consumption, there is also some conflicting evidence, as studies have demonstrated high false-negative rates of intraoperative frozen-section analysis—potentially resulting in unjustified nerve-sparing surgery (*6,7*).

For PC, PET/CT molecular imaging with radiopharmaceuticals targeting prostate-specific membrane antigen (PSMA) has been established in recent years. PSMA PET/CT is used for highly specific oncologic diagnostic imaging, especially in the setting of biochemical recurrence (*8–12*). Interestingly, PET imaging agents also emit optical photons via a phenomenon called Cerenkov luminescence. This property enables optical imaging, called Cerenkov luminescence imaging (CLI), using the novel LightPath system (Lightpoint Medical Ltd.) (*13*). Cerenkov photons are emitted by a charged particle (e.g., positron or electron) when traveling through a dielectric medium at a faster speed than the velocity of light in that medium (*13,14*). Although Cerenkov luminescence has a broad wavelength spectrum, it predominantly comprises ultraviolet light and blue light. These short wavelengths are highly attenuated in biologic tissue. Therefore, CLI is limited to the detection of signals emitted in superficial tissue layers. In contrast to PET, CLI is unable to detect photons emitted by more deeply located tissues or

Received Sep. 6, 2021; revision accepted Nov. 30, 2021.
For correspondence or reprints, contact Pedro Fragoso Costa (pedro.fragoso-costa@uni-duisburg-essen.de) and Christopher Darr (christopher.darr@uk-essen.de).
Published online Dec. 16, 2021.

tumors (*15,16*). Intraoperative imaging with CLI is promising because it allows evaluation of the entire surface of the prostate, whereas intraoperative frozen-section analysis includes only a limited number of prostatic slices and thus is susceptible to sampling errors. Initial feasibility studies for intraoperative use in PC show promising results. So far, these have been based on small patient cohorts and selected patients, mainly with intermediate- to high-risk PC. One difference between the studies is the number of injections. In Olde Heuvel et al. (*17*), preoperative PET/CT was performed 4 wk before surgery with intraoperative tracer injection, whereas Darr et al. (*18*) examined immediate preoperative PET/CT without intraoperative tracer injection.

CLI could significantly improve the oncologic outcome of this patient group in the future; however, the safety of the medical staff must also be guaranteed and ensured. Radiation exposure has been thoroughly evaluated for sentinel lymph node procedures with ^{99m}Tc-labeled compounds and has shown consistent values of exposure from 1 to 10 μSv (*19–22*) per procedure. However, PET tracers carry an inherent risk of additional radiation exposure because of the higher energy and number of annihilation γ-photons in comparison to the γ-photons from ^{99m}Tc (*23*). Olde Heuvel et al. presented first data with a maximum radiation exposure of 0.016 mSv per procedure as the radiation exposure of medical personnel from 5 patients undergoing CLI-guided RP after intraoperative ^{68}Ga-PSMA-11 administration (*17*).

To calculate a possible scenario for radiation exposure in a new situation, such as radioguided surgery using positron emitters, medical physicists must rely on evidence-based publications. However, these are mostly available for different situations, such as clinical technologist exposure from patients undergoing PET/CT imaging or metrological data—which is either theoretically determined or measured in very controlled situations not corresponding to a realistic clinical operation (*24,25*). *Exposure limits must be observed and, if necessary, the operation theater must be reclassified as a temporary radiation-controlled area.*

The objective of this study was to provide a quantitative description of the total additional occupational exposure that would occur for surgery personnel and pathologists from patients undergoing preoperative ^{68}Ga-PSMA PET/CT and subsequent radioguided RP.

MATERIALS AND METHODS

Surgery and Intraoperative CLI

Ten patients with preoperative ^{68}Ga-PSMA-11 administration and intraoperative CLI were included in the present radiation exposure study (5 of whom were included for post-PET/CT γ-field dose rate investigations). The work flow of our "1-stop-shop" protocol is shown in Figure 1. Patients received 141.9 ± 57.86 (average ± SD) MBq of ^{68}Ga-PSMA-11 for PET/CT, in accordance with guideline recommendations (*26*). After ^{68}Ga-PSMA PET/CT, radioguided RP was performed. A urinary catheter was inserted in the operating room to drain the urine. The excised prostate specimen was immediately retrieved from the abdomen, wiped to clear blood and fluids, positioned in a specimen tray, and then imaged with the LightPath system. After the imaging was done, the prostate gland was assessed for radioactivity quantification with a germanium detector.

Patient Dose Rate

An initial evaluation of the detector response consisted of 3 measurements of a point source of 60 MBq using a proportional counter–based dose rate meter (FH 40 G-L; Thermo Fisher Scientific); all measurements included background subtraction.

Subsequently, we evaluated the impact of patient orientation toward the radiation detector, compared with a point source, and later provided a rough estimation of the fraction of tracer elimination until prostatectomy. For this step, we obtained measurements from 10 patients

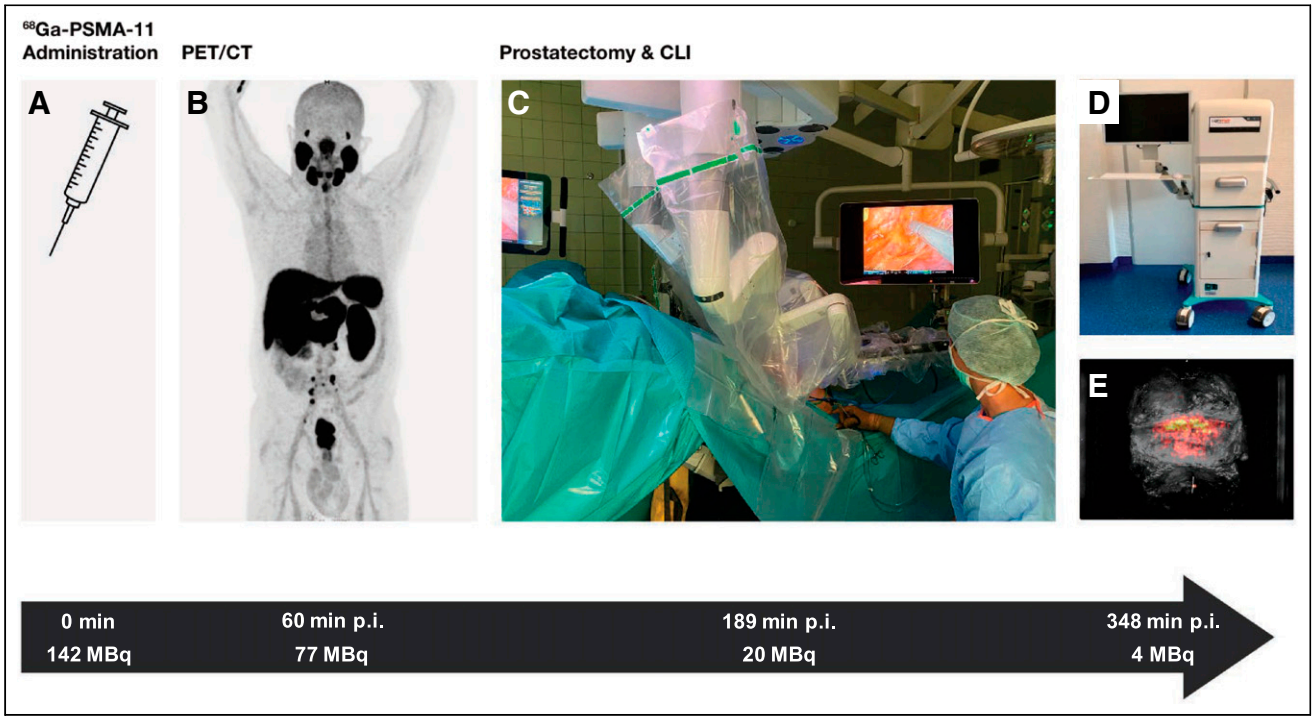

FIGURE 1. One-stop-shop protocol, including tracer administration (A), PET/CT imaging (B), and CLI during prostatectomy (C–E), permitted by remainder of ^{68}Ga-PSMA-11 uptake in prostate. Temporal sequence (black arrow) shows median time points after injection (p.i.) and decay-corrected whole-body activity expected for each step of protocol.

injected with ^{68}Ga-PSMA-11 (10.4 ± 4.6 min after injection), in the standing position facing the right and left sides of the waist, with the condition that the patients did not eliminate any tracer via urine excretion (pre-PET/CT). At 100.2 ± 27.5 min after ^{68}Ga-PSMA-11 PET/CT scanning, measurements were obtained from 5 patients in the supine position (post-PET/CT). In total, 4 predefined positions were measured (coded as head [A], right side of the waist [B], left side of the waist [C], and feet [D]) at a distance of 1 m. These predefined positions corresponded to the locations around the patient where staff members (e.g., scrub nurse, surgical assistant) were likely to be in stationary positions during surgery including CLI. In total, 20 individual measurements were obtained.

The measured dose rates were plotted as a function of the injected tracer activity decay corrected to the time of the measurement, and a linear fit (least squares method) was applied, constraining the fit to pass at the origin (i.e., the condition in which there is no tracer; the dose rate output will be equal to that measured as the background signal). We postulated that the slope of the fit would provide an estimate of the patient-specific dose rate constant at the defined positions.

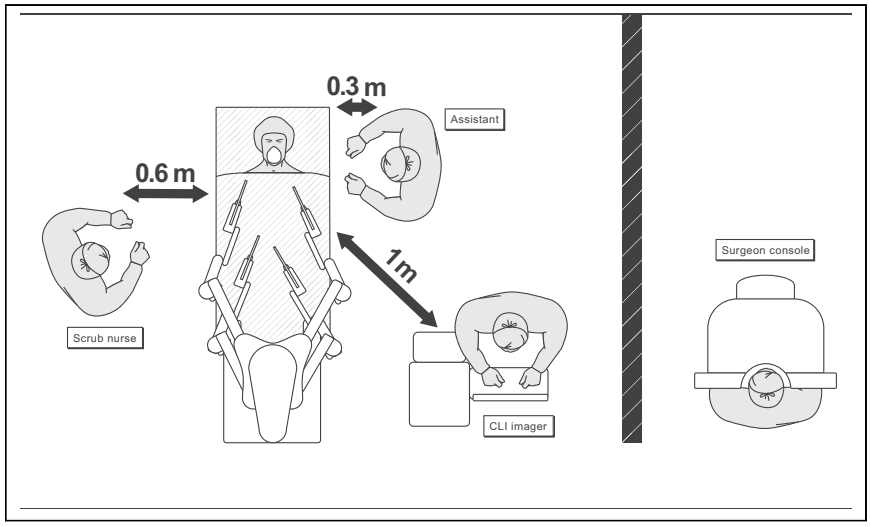

FIGURE 2. Setup in operating theater and respective distances used for calculated personal equivalent doses based on patient-specific dose rate constants.

Electronic Personal Dosimetry (EPD)

The exposure of the medical personnel was assessed in 10 procedures using EPD. RAD-60 (Mirion Technologies) dosimeters were positioned at waist level. Measurements included the first surgical assistant and scrub nurse at the operating table and the CLI imager/surgeon at the robotic console and encompassed the whole duration of surgery.

EPD Versus Dose Rate Predictions

On the basis of the different patient-specific dose rate constants at the defined positions, the exposure during the procedure was calculated as:

$$\dot{H}^{*}(10) = \frac{\Gamma_{H^{*}} \cdot A}{r^{2}} \cdot RF, \qquad \text{Eq. 1}$$

where $\dot{H}^{*}(10)$ is the ambient dose equivalent rate at a 10-mm depth, and $\Gamma_{H^{*}}$ is the dose rate constant. A is the radionuclide activity, and r is the distance from the source to the detector. Because ^{68}Ga is a short-lived radionuclide (half-life value of 67.71 min), the activity present in a given sample will decrease as a function of the time of measurement, thus causing a decrease in the dose rate. Taking this phenomenon into account, we introduced a correction factor that was obtained by integrating the dose rate over the measured time (t); this factor was referred to as a reduction factor (*25*):

$$RF = 1.433 \cdot \frac{T_{1/2}}{t} \cdot \left(1 - \exp\left[\frac{0.693 \cdot t}{T_{1/2}}\right]\right). \qquad \text{Eq. 2}$$

Because operating room personnel are mostly stationary in robot-assisted surgery, it is reasonable to assume that the point source exposure modeling will provide a reasonable estimation. If we measure the typical distance from the source to the exposed first assistant, scrub nurse, and CLI imager (Fig. 2), we find that r is equal to 0.3, 0.6, and 1 m, respectively (the CLI imager is also a conservative surrogate for the anesthetist and the primary surgeon at the console). To accommodate any uncertainty related to the exact position of each health care professional, 2 additional points at ±10 cm of the reference position were considered. The health care professional positions were then superimposed on Figure 3, such that the first surgical assistant and the CLI imager/surgeon were attributed the dose rate value corresponding to position C, whereas the scrub nurse was attributed that corresponding to position B.

Prostate Gland Specimens

To access the tracer activity present in the prostate gland, as an indicator for the pathologist's skin exposure, 8 prostate specimens were measured with a Hyper-Pure germanium detector (HPGe) (Canberra) after prostate excision and CLI. To ensure adequate pathologic processing afterward, the specimens had already been placed in formalin. The radiation measurement was performed using a 20-min protocol,

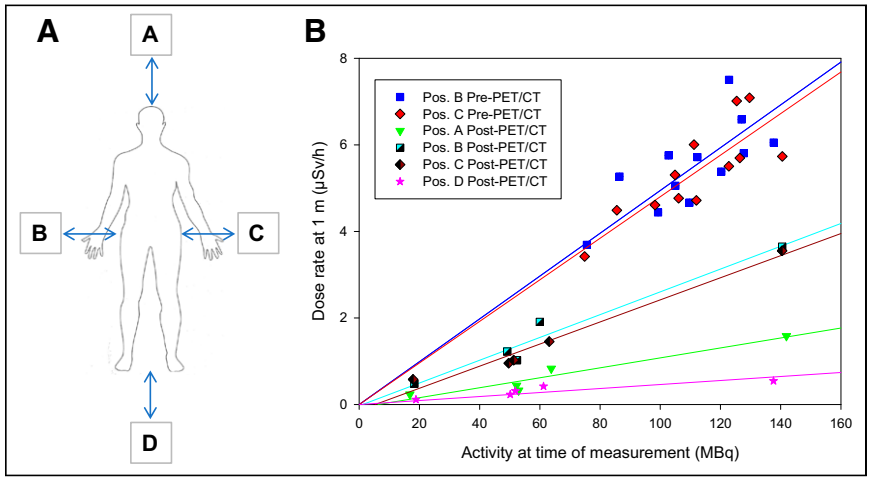

FIGURE 3. Dose rate measurements at predefined positions (Pos.) (A) and respective linear regression lines (B). Positions are as follows: A = at head; B = right side; C = left side; D = at feet. Post-PET/CT = dose rate readings immediately before entering operating room; Pre-PET/CT = measurements immediately after tracer injection.

TABLE 1
Summary of Dose Rate Measurements, Activity at Time of Measurement, and Respective Patient-Specific Dose Rate Constants (Dose Rate/Activity)

Position	Activity, MBq		Dose Rate/Activity, $\mu Sv \cdot h^{-1} \cdot MBq^{-1}$		
	Average	SD	Average	SD	r^2
Point source (1 m)	69.96	2.3	0.145	0.002	
Patient before PET (1 m)	112.2	17.7			
B			0.047	0.004	0.70
C			0.047	0.005	0.66
Patient after PET (1 m)	64.5	41.7			
A			0.011	0.003	0.92
B			0.026	0.004	0.96
C			0.024	0.005	0.97
D			0.003	0.004	0.84

followed by an automatic sequence for the identification of the 511-keV energy peak and further quantification based on energy and efficiency calibration curves.

The detected activity for HPGe provided an estimate of the exposure of the pathologists who performed frozen-section procedures. As a threshold, we used nuclide-specific exemption limits (^{68}Ga < 100 kBq) (*27*).

Because not all centers may have access to HPGe detectors, we present an alternative method for accessing the amount of radiotracer present in the excised specimen on the basis of ^{68}Ga-PSMA-11 imaging. The method consists of defining a region delimited by the prostate anatomic boundaries on the basis of CT imaging. The same volume is then overlaid on the PET reconstructed images to provide an estimate of the total amount of tracer.

RESULTS

Patient Dose Rate

Initial measurements around the patient showed a decreased dose rate constant compared with a point source. The measured dose rate values averaged 5.3 ± 0.9 μSv/h. If a linear relationship between the dose rate and tracer activity (decay corrected to the time of measurement) is assumed, then the patient-specific dose rate constant for each measured position can be extracted, showing both position B ($n = 10$) and position C ($n = 10$): 0.047 μSv/h·MBq versus 0.145 ± 0.002 μSv/h·MBq for the point source (Table 1).

The dose rate measurements immediately before surgery (post-PET/CT) averaged 1.04 ± 1.00 μSv/h (minimum: 0.115 μSv/h; maximum, 3.65 μSv/h). The lowest dose rates were detected at the head and the feet of the patients. The patient-specific dose rate constant values obtained from a linear modulation were 0.011, 0.026, 0.024, and 0.003 μSv/h·MBq, corresponding to the head (A), right waist (B), left waist (C), and feet (D), respectively.

Patient Demographics and Oncologic Data

Patient characteristics are displayed in Table 2. In total, 10 patients with histologically confirmed PC were included; of those, 50% had locally advanced disease and 50% had high-risk PC. The median time from tracer injection until CLI was 328.5 min (interquartile range [IQR], 298.75–371.75 min). This study received formal ethics committee approval (19–8749-BO), and all subjects provided written informed consent.

EPD

For the 10 procedures considered, the average EPD monitoring duration was 242 ± 14 min, starting 189 ± 38 min after ^{68}Ga-PSMA-11 administration. EPD readings revealed average personal equivalent doses [Hp(10)] of 9.0 ± 7.1, 3.3 ± 3.9, and 0.7 ± 0.7 μSv for first surgical assistant, scrub nurse, and CLI imager/surgeon at the robotic console, respectively.

EPD Versus Dose Rate Predictions

Regarding the calculated Hp(10) based on patient-specific dose rate constants, we observed average Hp(10) of 11.7 ± 10.0, 2.7 ± 1.7, and 0.8 ± 0.5 μSv for the first surgical assistant, scrub nurse, and CLI imager/surgeon, respectively. These values correspond to success rates (the condition in which the read EPD falls within the ±10-cm uncertainty–calculated exposure) of 90%, 40%, and 20% for the first surgical assistant, scrub nurse, and CLI imager/surgeon, respectively. The procedure-specific values for exposure are shown in Figure 4.

Prostate Gland Specimens

Prostate gland specimens were excised and analyzed by CLI at medians of 348 min (IQR, 282–437 min) after ^{68}Ga-PSMA-11 administration and 276 min (IQR, 194–369 min) after PET/CT imaging. The measurements with the HPGe were obtained 71 min (IQR, 42–143 min) after prostate excision. All activity values were decay corrected to the time of prostate excision.

HPGe measurements revealed activities between 0.9 and 38.6 kBq for ^{68}Ga. The median HPGe measured activity was 2.96 kBq (IQR, 2.23–7.65 kBq), whereas the median total activity encompassed in the prostate region PET reconstructed images accounted for 3.83 kBq (IQR, 2.83–8.50 kBq).

The deviation between HPGe values and PET activity values was characterized by a systematic overestimation (median of 18.9%) of PET activity values compared with HPGe values, as depicted in Figure 5. There were no statistical differences between HPGe and PET datasets with regard to prostate activity levels ($P = 0.090$).

DISCUSSION

In the present study, we were able to provide a systematic evaluation of the patient as a radioactive source in each of the different procedural steps encountered in PET/CT imaging and subsequent CLI for the evaluation of surgical margins during robot-assisted

TABLE 2
Demographic and Oncologic Data for 10 Patients

Characteristic	Value
Patient and imaging*	
Age, in y	63 (56.5–69)
BMI, in kg/m^2	30.37 (24.25–34.68)
Injected activity, in MBq	122 (99.25–185)
Activity derived from HPGe, in kBq/mL, corrected to time of excision	2.96 (2.24–7.65)
Activity derived from PET/CT in prostate, in kBq/mL, corrected to time of excision	3.83 (2.83–8.50)
Duration from tracer injection to CLI, in min	328.5 (298.75–371.75)
Duration from skin incision to CLI, in min	130.2 (125.4–145.2)
Surgical and oncologic†	
Organ-confined PC	5 (50)
Locally advanced PC	5 (50)
Initial PSA, in ng/mL*	12.5 (8.3–15.25)
Risk stratification according to D'Amico (*34*)	
Intermediate-risk PC	5 (50)
High-risk PC	5 (50)
ISUP-GGG	
2	4 (40)
3	4 (40)
4	0
5	2 (20)
Prostate specimen weight, in g*	43.5 (41.25–55)

*Reported as medians, with interquartile ranges in parentheses.
†Reported as numbers of patients, with percentages in parentheses, unless otherwise indicated.
BMI = body mass index; PSA = prostate-specific antigen; ISUP-GGG = International Society of Urological Pathology Gleason grading group.

prostatectomy for a single administration protocol (i.e., 1-stop-shop protocol) (Fig. 1). For this purpose, methods for prospective and department planning radiation protection calculations for this entirely new application of ^{68}Ga-PSMA-11 were used and included a point source exposure calculation and a reduction factor expected for long exposures to short-lived radionuclides.

In the first step of the present study, a measurement was elected to illustrate how the point source exhibits a similar dose rate per unit of activity at a 1-m distance. The resulting dose rate at 1 m normalized for activity showed a good concordance with the DIN (Deutsches Institut für Normung [German Institute for Standardisation Registered Association]) tabulated value of 0.1581 (0.145 measured) $\mu Sv \cdot h^{-1} \cdot MBq^{-1}$ for ^{68}Ga. The observed discrepancy was mainly due to a decreased detector responsivity to 511 keV, compared with the calibration γ-lines of ^{137}Cs (661.6 keV). However, for patients, partially because of self-attenuation (*28*), a discrepancy between tabulated values and those based on dose rate meter measurements was observed (Table 1). The positioning of the dose rate meter at a distance of 1 m from the radiation source, with a height greater than this distance, will result in a lower dose rate than that of a point source (*29*). Dose rate measurements performed after the PET/CT scan showed a decreased dose rate constant because much of the tracer had been excreted at this point, leading to a decrease in dose rate constants of approximately 50% compared with the values immediately after tracer injection (i.e., pre-PET/CT).

Despite being a simple and limited method, the point source approximation using patient-specific dose rate constants provided a plausible approximation for the occupational exposure measured by dosimeters, especially for the position of the assistant surgeon because a relaxation of $\pm$10 cm in the stationary condition could predict 90% of the measured doses. The greatest impairment of the dose estimation was due to very low exposure levels, illustrated by the CLI imager/surgeon position, for which most values of exposure were found to be between 0 and 1 μSv; these data suggested that the limiting factor was the lack of accuracy of EPD for measurements below the measuring range (1 μSv–9.99 Sv). The remainder of outliers could be explained by a higher proximity to the source or orientation of the dosimeter toward the radiation field outside the efficient angular range of EPD.

With respect to the measured Hp(10), it is evident from Equation 2 that the professional who operated nearest to the patient would have the highest exposure. Considering the general public exposure limit of 1 mSv as a threshold, that professional with the highest exposure (the first surgical assistant) (Fig. 4A) would be able to perform CLI after ^{68}Ga-PSMA-11 PET/CT for 110 radioguided RP procedures per year.

The presented "1-stop-shop" single administration for both PET/CT and CLI has been validated in a feasibility study (*18*) and serves as an example of the ALARA (as low as reasonably achievable) principle for radiation exposure optimization applied to radioguided

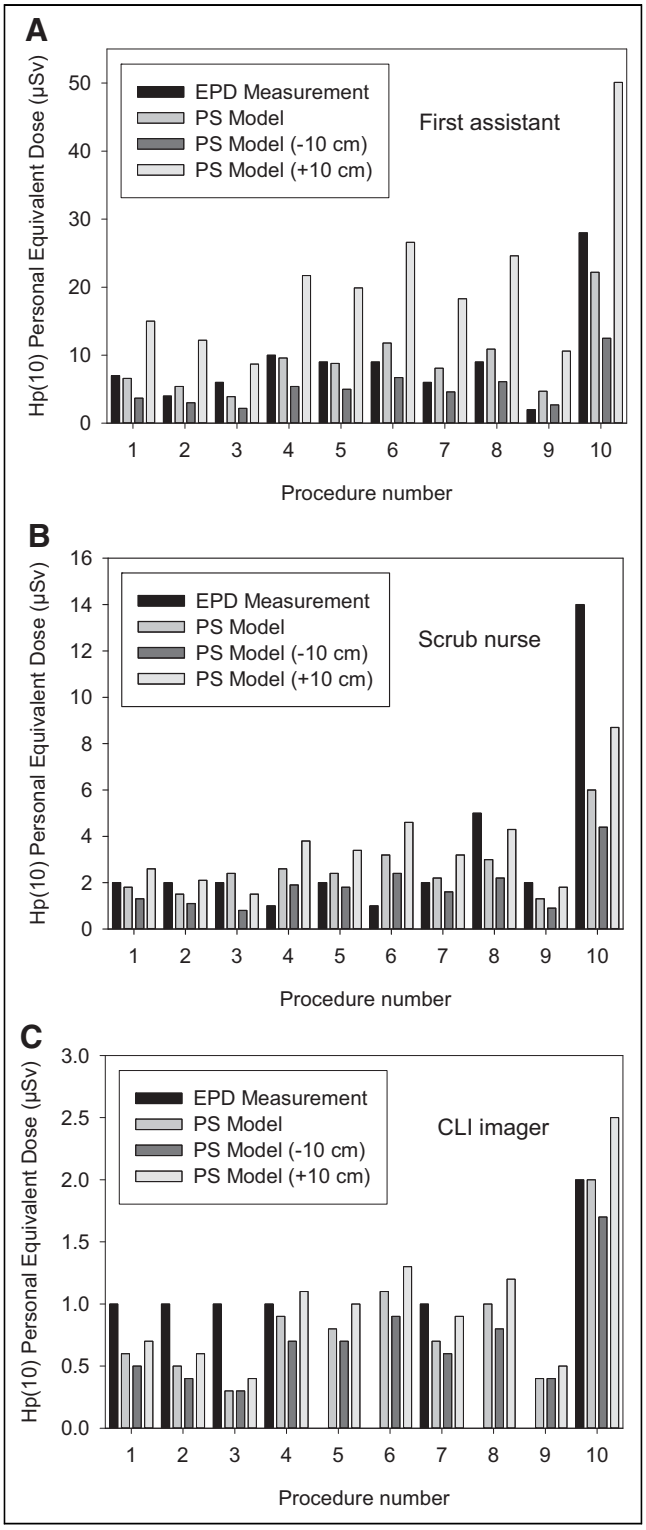

FIGURE 4. EPD measurements (black bars) alongside computed values based on point source (PS) model (medium gray bars) at measured distance *r*. Variations of minus −10 cm (dark gray bars) and +10 cm (light gray bars) from distance r using PS assumption are shown.

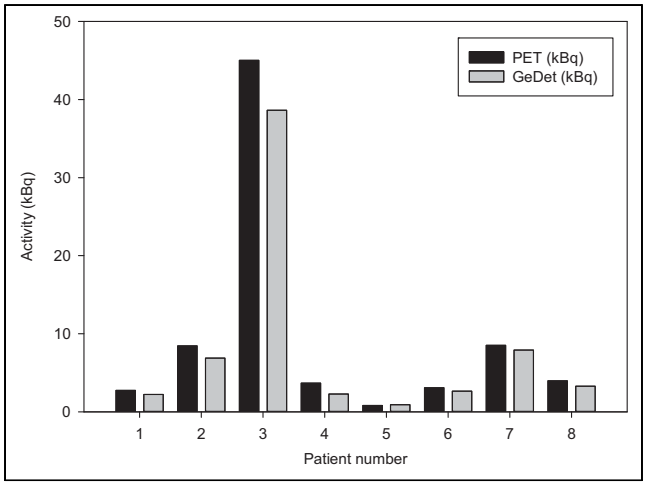

FIGURE 5. Activity quantification of excised prostate specimens decay corrected to time of excision. Black bars represent PET-based quantification (median, 3.83 kBq; IQR, 2.83–8.50 kBq). Gray bars represent HPGe measurement (GeDet) (median, 2.96 kBq; IQR, 2.23–7.65 kBq).

surgery—not only for the medical exposure of the patient by relinquishing a dedicated tracer injection of about 100 MBq, resulting in a patient effective dose of 2 mSv, but also by effectively decreasing the occupational exposure of the medical personnel. In a ^{68}Ga-PSMA-11 CLI primary prostate cancer study (*18*), with perioperative radiotracer administration of 100 MBq, an Hp(10) of 16 μSv was recorded for the most exposed medical professional. The data presented were for the sterile scrub nurse and were comparable to our collected data. However, no other exposure data were collected from other staff roles. According to our findings, the exposure values for the scrub nurse were quite variable, with an average Hp(10) of 3.3 ± 3.9 μSv, whereas the exposure values for the assistant were very precise and therefore more informative.

Other intraoperative CLI applications include the use of 2-^{18}F-FDG for the identification of surgical margins in breast-conserving surgery. From published studies, there is evidence that the preoperative administration of about 300 MBq of 2-^{18}F-FDG would deliver maximal personal equivalent doses of 34.0–61.8 μSv (*15,30*). Interestingly, when the ^{18}F decay characteristics and the assumption of the administration of 300 MBq were substituted in our model, then we obtained exposure levels of 51.3, 15.3, and 4.6 μSv per procedure for the first surgical assistant, scrub nurse, and surgeon, respectively.

CLI has been important in preclinical evaluations of disease models using several β-emitters, mostly because of the small dimensions of the image samples (mostly from mice), which are favorable for CLI, and the cost-efficiency compared with preclinical PET/CT scanners. With translation in the intraoperative environment, it is conceivable that new radionuclides (such as the longer-lived ^{89}Zr or ^{64}Cu) will become relevant in CLI-radioguided surgery; for these radionuclides, our exposure model could provide some insight in terms of predicting occupational exposures (*31*).

Our approach for the pathologist's exposure was a conservative surrogate for a direct measurement of exposure with a ring dosimeter; we directly measured the activity contained in the prostate gland using the HPGe. On the basis of our data, there was no significant radiation exposure to pathology staff. Additionally, we provided an independent measurement based on PET data obtained before CLI. Our results indicated a systematic overestimation of the activity levels found by PET in comparison with the HPGe. The systematic result suggests that this method of tracer amount estimation may be limited by the presence of activity in surrounding tissues, namely, the bladder, that would overestimate the radioactivity content in the prostate specimen. However, with the exception of

1 specimen, the PET estimate could predict the HPGe value below 10% error. Various standardized exposure situations are given in the literature. Delacroix et al. described hand contact on a glass beaker filled with 50 mL of ^{68}Ga solution (*27*). With this method, a dose of approximately 4 μSv would be expected from a 1-h contact. This specification is consistent with our results, considering the 50-mSv radiation exposure limit to the skin for members of the public (*32*).

The present study has several limitations. First, our study was related to the low radiation field that provides poor statistics for counting devices. This limitation also translates to difficulty for the point source model in predicting such low exposures. Second, the fact that we used point source geometry is also a limitation, as in real life the patient is not a point source. Further studies using anthropomorphic mathematic phantoms as the source of external exposure could address this limitation (*33*). Finally, we did not provide measured evidence of skin exposure by means of a ring dosimeter and therefore could not directly correlate the activity levels in the specimen with the finger exposure of the histopathology staff.

CONCLUSION

The single-injection PET/CT CLI-guided RP protocol can be performed in about 110 procedures per year before the limit for public radiation exposure is reached. All prostate specimen radionuclide content was below the exemption level for ^{68}Ga at the time of excision. Overall, the occupational risk of the 1-stop-shop protocol appears to be quite low, meaning that it is not necessary to reclassify the operation theater as a temporary radiation-controlled area. Furthermore, no radiation safety measures are required for specimen handling in the pathology department. Further validation for other radionuclides with the potential for CLI-radioguided surgery or other types of radioguided surgery, such as ^{18}F-PSMA-1007, should be addressed in future studies.

DISCLOSURE

Boris A. Hadaschik has had advisory roles for ABX, Astellas, AstraZeneca, Bayer, Bristol Myers Squibb, Janssen R&D, Lightpoint Medical Ltd., and Pfizer; has received research funding from Astellas, Bristol Myers Squibb, German Research Foundation, Janssen R&D, and Pfizer; and has received compensation for travel from Astellas, AstraZeneca, and Janssen R&D. Wolfgang P. Fendler reports fees from BTG (consultant), Calyx (consultant), RadioMedix (PET reader), Bayer (speakers bureau), and Parexel (image reader) outside the submitted work. Ken Herrmann reports personal fees from Bayer, personal fees from Sofie Biosciences, personal fees from SIRTEX, nonfinancial support from ABX, personal fees from Adacap, personal fees from Curium, personal fees from Endocyte, grants and personal fees from BTG, personal fees from IPSEN, personal fees from Siemens Healthineers, personal fees from GE Healthcare, personal fees from Amgen, personal fees from Novartis, personal fees from ymabs, personal fees from Aktis Oncology, personal fees from Theragnostics, and personal fees from Pharma15 outside the submitted work. Ken Herrmann is an associate editor of *JNM*. Maarten R. Grootendorst is an employee of Lightpoint Medical Ltd. No other potential conflict of interest relevant to this article was reported.

ACKNOWLEDGMENTS

We thank the technologists of the nuclear medicine teams and the nurses of the urology surgery teams for their ongoing logistic support.

KEY POINTS

QUESTION: What is the radiation exposure risk for CLI-radioguided surgery after ^{68}Ga-PSMA-11 administration for surgery personnel?

PERTINENT FINDINGS: The protocol can be performed at about 110 procedures per year before the limit for public radiation exposure is reached.

IMPLICATIONS FOR PATIENT CARE: Implementation of CLI-radioguided surgery procedures does not involve additional radioprotection hurdles.

REFERENCES

1. *EAU Guidelines*. Edn. presented at the EAU Annual Congress Amsterdam 2022. EAU Guidelines Office. European Association of Urology website. https://uroweb.org/guidelines. Accessed August 9, 2022.
2. Martini A, Gandaglia G, Fossati N, et al. Defining clinically meaningful positive surgical margins in patients undergoing radical prostatectomy for localised prostate cancer. *Eur Urol Oncol.* 2021;4:42–48.
3. Gandaglia G, Ploussard G, Valerio M, et al. The key combined value of multiparametric magnetic resonance imaging, and magnetic resonance imaging–targeted and concomitant systematic biopsies for the prediction of adverse pathological features in prostate cancer patients undergoing radical prostatectomy. *Eur Urol.* 2020;77:733–741.
4. Radtke JP, Hadaschik BA, Wolf MB, et al. The impact of magnetic resonance imaging on prediction of extraprostatic extension and prostatectomy outcome in patients with low-, intermediate- and high-risk prostate cancer: try to find a standard. *J Endourol.* 2015;29:1396–1405.
5. Petralia G, Musi G, Padhani AR, et al. Robot-assisted radical prostatectomy: multiparametric MR imaging–directed intraoperative frozen-section analysis to reduce the rate of positive surgical margins. *Radiology.* 2015;274:434–444.
6. Schlomm T, Tennstedt P, Huxhold C, et al. Neurovascular structure-adjacent frozen-section examination (NeuroSAFE) increases nerve-sparing frequency and reduces positive surgical margins in open and robot-assisted laparoscopic radical prostatectomy: experience after 11,069 consecutive patients. *Eur Urol.* 2012;62:333–340.
7. Gillitzer R, Thüroff C, Fandel T, et al. Intraoperative peripheral frozen sections do not significantly affect prognosis after nerve-sparing radical prostatectomy for prostate cancer. *BJU Int.* 2011;107:755–759.
8. Perera M, Papa N, Roberts M, et al. Gallium-68 prostate-specific membrane antigen positron emission tomography in advanced prostate cancer: updated diagnostic utility, sensitivity, specificity, and distribution of prostate-specific membrane antigen-avid lesions—a systematic review and meta-analysis. *Eur Urol.* 2020;77:403–417.
9. Yaxley JW, Raveenthiran S, Nouhaud FX, et al. Risk of metastatic disease on ^{68}gallium-prostate-specific membrane antigen positron emission tomography/computed tomography scan for primary staging of 1253 men at the diagnosis of prostate cancer. *BJU Int.* 2019;124:401–407.
10. Koschel S, Murphy DG, Hofman MS, Wong L-M. The role of prostate-specific membrane antigen PET/computed tomography in primary staging of prostate cancer. *Curr Opin Urol.* 2019;29:569–577.
11. Kalapara AA, Nzenza T, Pan HYC, et al. Detection and localisation of primary prostate cancer using ^{68}gallium prostate-specific membrane antigen positron emission tomography/computed tomography compared with multiparametric magnetic resonance imaging and radical prostatectomy specimen pathology. *BJU Int.* 2020;126:83–90.
12. Morris MJ, Carroll PR, Saperstein L, et al. Impact of PSMA-targeted imaging with ^{18}F-DCFPyL-PET/CT on clinical management of patients (pts) with biochemically recurrent (BCR) prostate cancer (PCa): results from a phase III, prospective, multicenter study (CONDOR). *Am J Clin Oncol.* 2020;38(suppl):5501.
13. Das S, Thorek DL, Grimm J. Cerenkov imaging. *Adv Cancer Res.* 2014;124:213–234.
14. Grootendorst MR, Cariati M, Kothari A, Tuch DS, Purushotham A. Cerenkov luminescence imaging (CLI) for image-guided cancer surgery. *Clin Transl Imaging.* 2016;4:353–366.
15. Grootendorst MR, Cariati M, Pinder SE, et al. Intraoperative assessment of tumor resection margins in breast-conserving surgery using ^{18}F-FDG Cerenkov luminescence imaging: a first-in-human feasibility study. *J Nucl Med.* 2017;58:891–898.

16. Chin PT, Welling MM, Meskers SC, Olmos RAV, Tanke H, van Leeuwen FW. Optical imaging as an expansion of nuclear medicine: Cerenkov-based luminescence vs fluorescence-based luminescence. *Eur J Nucl Med Mol Imaging.* 2013;40:1283–1291.
17. Olde Heuvel J, van der Poel HG, Bekers EM, et al. ^{68}Ga-PSMA Cerenkov luminescence imaging in primary prostate cancer: first-in-man series. *Eur J Nucl Med Mol Imaging.* 2020;47:2624–2632.
18. Darr C, Harke NN, Radtke JP, et al. Intraoperative ^{68}Ga-PSMA Cerenkov luminescence imaging for surgical margins in radical prostatectomy: a feasibility study. *J Nucl Med.* 2020;61:1500–1506.
19. Bekiş R, Celik P, Uysal B, et al. Exposure of surgical staff to radiation during surgical probe applications in breast cancer. *J Breast Cancer.* 2009;12:27–31.
20. Klausen TL, Chakera A, Friis E, Rank F, Hesse B, Holm S. Radiation doses to staff involved in sentinel node operations for breast cancer. *Clin Physiol Funct Imaging.* 2005;25:196–202.
21. Waddington WA, Keshtgar M, Taylor I, Lakhani S, Short M, Eli P. Radiation safety of the sentinel lymph node technique in breast cancer. *Eur J Nucl Med.* 2000;27:377–391.
22. Brenner W, Ostertag H, Peppert E, et al. Radiation exposure to the personnel in the operating room and in the pathology due to SLN detection with Tc-99m-nanocolloid in breast cancer patients. *Nuklearmedizin.* 2000;39:142–145.
23. Heckathorne E, Dimock C, Dahlbom M. Radiation dose to surgical staff from positron-emitter-based localization and radiosurgery of tumors. *Health Phys.* 2008;95:220–226.
24. Costa PF, Reinhardt M, Poppe B. Occupational exposure from F-18-FDG PET/CT: implementation to routine clinical practice. *Radiat Prot Dosimetry.* 2018;179:291–298.
25. Madsen MT, Anderson JA, Halama JR, et al. AAPM task group 108: PET and PET/CT shielding requirements. *Med Phys.* 2006;33:4–15.
26. Fendler WP, Eiber M, Beheshti M, et al. ^{68}Ga-PSMA PET/CT: joint EANM and SNMMI procedure guideline for prostate cancer imaging: version 1.0. *Eur J Nucl Med Mol Imaging.* 2017;44:1014–1024.
27. Delacroix D, Guerre JP, Leblanc P, Hickman C. Radionuclide and radiation protection data handbook 2nd edition (2002). *Radiat Prot Dosimetry.* 2002;98:9–168.
28. Zeff BW, Yester MV. Patient self-attenuation and technologist dose in positron emission tomography. *Med Phys.* 2005;32:861–865.
29. Yi Y, Stabin M, McKaskle M, Shone M, Johnson A. Comparison of measured and calculated dose rates near nuclear medicine patients. *Health Phys.* 2013;105:187–191.
30. Jurrius PA, Grootendorst MR, Krotewicz M, et al. Intraoperative [^{18}F]FDG flexible autoradiography for tumour margin assessment in breast-conserving surgery: a first-in-human multicentre feasibility study. *EJNMMI Res.* 2021;11:28.
31. Collamati F, van Oosterom MN, Hadaschik BA, et al. Beta radioguided surgery: towards routine implementation? *Q J Nucl Med Mol Imaging.* 2021;65:229–243.
32. The 2007 Recommendations of the International Commission on Radiological Protection. ICRP publication 103. *Ann ICRP.* 2007;37:1–332.
33. Xu XG. An exponential growth of computational phantom research in radiation protection, imaging, and radiotherapy: a review of the fifty-year history. *Phys Med Biol.* 2014;59:R233–R302.
34. D'Amico AV, Whittington R, Malkowicz SB, et al. Biochemical outcome after radical prostatectomy, external beam radiation therapy, or interstitial radiation therapy for clinically localized prostate cancer. *JAMA* 1998;280:969–974.